

See discussions, stats, and author profiles for this publication at: <https://www.researchgate.net/publication/344335066>

Explicit solution simulation method for the $3/2$ model

Preprint · September 2020

CITATIONS

0

READS

67

3 authors, including:



Michael A. Kouritzin

University of Alberta

93 PUBLICATIONS 574 CITATIONS

SEE PROFILE

EXPLICIT SOLUTION SIMULATION METHOD FOR THE 3/2 MODEL

IRO RENÉ KOUARFATE, MICHAEL A. KOURITZIN, AND ANNE MACKAY

ABSTRACT. An explicit weak solution for the 3/2 stochastic volatility model is obtained and used to develop a simulation algorithm for option pricing purposes. The 3/2 model is a non-affine stochastic volatility model whose variance process is the inverse of a CIR process. This property is exploited here to obtain an explicit weak solution, similarly to Kouritzin (2018) for the Heston model. A simulation algorithm based on this solution is proposed and tested via numerical examples. The performance of the resulting pricing algorithm is comparable to that of other popular simulation algorithms.

1. INTRODUCTION

Recent work by Kouritzin (2018) shows that it is possible to obtain an explicit weak solution for the Heston model, and that this solution can be used to simulate asset prices efficiently. Exploiting the form of the weak solution, which naturally leads to importance sampling, Kouritzin and MacKay (2020) suggest the use of sequential sampling algorithms to reduce the variance of the estimator, inspired by the particle filtering literature. Herein, we show that the main results of Kouritzin (2018) can easily be adapted to the 3/2 stochastic volatility model and thus be exploited to develop an efficient simulation algorithm that can be used to price exotic options.

The 3/2 model is a non-affine stochastic volatility model whose analytical tractability was studied in Heston (1997) and Lewis (2000). A similar process was used in Ahn and Gao (1999) to model stochastic interest rates. Non-affine stochastic volatility models have been shown to provide a good fit to empirical market data, sometimes better than some affine volatility models; see Bakshi et al. (2006) and the references provided in the literature review section of Zheng and Zeng (2016). The 3/2 model in particular is preferred by Carr and Sun (2007) as it naturally emerges from consistency requirements in their proposed framework, which models variance swap rates directly.

As a result of the empirical evidence in its favor, and because of its analytical tractability, the 3/2 model has gained traction in the academic literature over the past decade. In particular, Itkin and Carr (2010) price volatility swaps and options

Key words and phrases. 3/2 model, explicit solutions, weak solutions, stochastic volatility, Monte Carlo simulations, option pricing, non-affine volatility.

Partial funding in support of this work was provided by an FRQNT grant and by NSERC discovery grants.

on swaps for a class of Levy models with stochastic time change and use the 3/2 model as a particular case. The 3/2 model also allows for analytical expressions for the prices of different volatility derivatives; see for example Drimus (2012), Goard and Mazur (2013) and Yuen et al. (2015). Chan and Platen (2015) consider the 3/2 model for pricing long-dated variance swaps under the real world measure. Zheng and Zeng (2016) obtain a closed-form partial transform of a relevant density and use it to price variance swaps and timer options. In Grasselli (2017), the 3/2 model is combined with the Heston model to create the new 4/2 model.

For the 3/2 model's growing popularity, there are very few papers that focus on its simulation. One of them is Baldeaux (2012), who adapts the method of Broadie and Kaya (2006) to the 3/2 model and suggests variance reduction techniques. The capacity to simulate price and volatility paths from a given market model is necessary in many situations, from pricing exotic derivatives to developing hedging strategies and assessing risk. The relatively small size of the literature concerning the simulation of the 3/2 model could be due to its similarity with the Heston model, which allows for easy transfer of the methods developed for the Heston model to the 3/2 one. Indeed, the 3/2 model is closely linked to the Heston model; the stochastic process governing the variance of the asset price in the 3/2 is the inverse of a square-root process, that is, the inverse of the variance process under Heston.

This link between the Heston and the 3/2 model motivates the present work; Kouritzin (2018) mentions that his method cannot survive the spot volatility reaching 0. Since the volatility in the 3/2 model is given by the inverse of a "Heston volatility" (that is, the inverse of a square-root process), it is necessary to restrict the volatility parameters in such a way that the Feller condition is met, in order to keep the spot volatility from exploding. In other words, by definition of the 3/2 model, the variance process always satisfies the Feller condition, which makes it perfectly suitable to the application of the explicit weak solution simulation method of Kouritzin (2018).

It is also worthwhile to note that Kouritzin and MacKay (2020) notice that the resulting simulation algorithm performs better when the Heston parameters keep the variance process further from 0. It is reasonable to expect that calibrating the 3/2 model to market data give such parameters, since they would keep the variance process (i.e. the inverse of the Heston variance) from reaching very high values. This insight further motivates our work, in which we adapt the method of Kouritzin (2018) to the 3/2 model.

As stated above, many simulation methods for the Heston model can readily be applied to the 3/2 model. Most of these methods can be divided into two categories; the first type of simulation schemes relies on discretizing the spot variance and the log-price process. Such methods are typically fast, but the discretization induces a bias which needs to be addressed, see Lord et al. (2010) for a good overview. Broadie and Kaya (2006) proposed an exact simulation scheme which relies on transition density of the variance process and an inversion of the Fourier transform of the integrated variance. While exact, this method is slow, and has thus prompted several authors to propose approximations and modifications to the original algorithm to

speed it up (see for example Andersen (2007)). Bégin et al. (2015) offers a good review of many existing simulation methods for the Heston model.

The simulation scheme proposed by Kouritzin (2018) for the Heston model relies on an explicit weak solution for the stochastic differential equation (SDE) describing the Heston model. This result leads to a simulation and option pricing algorithm which is akin to importance sampling. Each path is simulated using an artificial probability measure, called the reference measure, under which exact simulation is possible and fast. The importance sampling price estimator is calculated under the pricing measure by multiplying the appropriate payoff (a function of the simulated asset price and volatility paths) by a likelihood, which weights each payoff proportionally to the likelihood that the associated path generated from the reference measure could have come from the pricing measure. The likelihood used as a weight in the importance sampling estimator is a deterministic function of the simulated variance process, and is thus easy to compute. The resulting pricing algorithm has been shown to be fast and to avoid the problems resulting from discretization of the variance process.

In this paper, we develop a similar method for the 3/2 model by first obtaining a weak explicit solution for the two-dimensional SDE. We use this solution to develop an option price importance estimator, as well as a simulation and option pricing algorithm. Our numerical experiments show that our new algorithm performs at least as well as other popular algorithms from the literature. We find that the parametrization of the model impacts the performance of the algorithm.

The paper is organized as follows. Section 2 contains a detailed presentation of the 3/2 model as well as our main result. Our pricing algorithm is introduced in Section 3, in which we also outline existing simulation techniques, which we use in our numerical experiments. The results of these experiments are given in Section 4, and Section 5 concludes.

2. SETTING AND MAIN RESULTS

We consider a probability space $(\Omega, \mathcal{F}, \mathbb{P})$, where \mathbb{P} denotes a pre-determined risk-neutral measure¹ for the 3/2 model. The dynamics of the stock price under this chosen risk-neutral measure are represented by a two-dimensional process $(S, V) = \{(S_t, V_t), t \geq 0\}$ satisfying

$$\begin{cases} dS_t &= rS_t dt + \sqrt{V_t}S_t \rho dW_t^{(1)} + \sqrt{V_t}S_t \sqrt{1 - \rho^2} dW_t^{(2)} \\ dV_t &= \kappa V_t(\theta - V_t) dt + \varepsilon V_t^{3/2} dW_t^{(1)}, \end{cases} \quad (2.1)$$

with $S_0 = s_0 > 0$ and $V_0 = v_0 > 0$, and where $W = \{(W_t^{(1)}, W_t^{(2)}), t \geq 0\}$ is a two-dimensional uncorrelated Brownian motion, r, κ, θ and ε are constants satisfying $\kappa > -\frac{\varepsilon^2}{2}$, and $\rho \in [-1, 1]$. The drift parameter r represents the risk-free rate and ρ represents the correlation between the stock price S and its volatility V .

¹Since our goal in this work is to develop pricing algorithms, we only consider the risk-neutral measure used for pricing purposes.

The restriction $\kappa > -\frac{\varepsilon^2}{2}$ imposed on the parameters keeps the variance process from exploding. This property becomes clear when studying the process $U = \{U_t, t \geq 0\}$ defined by $U_t = \frac{1}{V_t}$ for $t \geq 0$. Indeed, it follows from Itô's lemma that

$$\begin{aligned} dU_t &= \kappa\theta \left(\frac{\kappa + \varepsilon^2}{\kappa\theta} U_t \right) dt - \varepsilon\sqrt{U_t} dW_t^{(1)} \\ &= \tilde{\kappa}(\tilde{\theta} - U_t) dt + \tilde{\varepsilon}\sqrt{U_t} dW_t^{(1)} \end{aligned}$$

where $\tilde{\kappa} = \kappa\theta$, $\tilde{\theta} = \frac{\kappa + \varepsilon^2}{\kappa\theta}$ and $\tilde{\varepsilon} = -\varepsilon$. In other words, with the restriction $\kappa > -\frac{\varepsilon^2}{2}$, U is a square-root process satisfying the Feller condition $\tilde{\kappa}\tilde{\theta} > \frac{\tilde{\varepsilon}^2}{2}$, so that $\mathbb{P}(U_t > 0) = 1$ for all $t \geq 0$.

In order to use results obtained for the Heston model and adapt them to the 3/2 model, we express (2.1) in terms of the inverse of the variance process, U , as follows

$$\begin{cases} dS_t &= rS_t dt + \sqrt{U_t^{-1}} S_t \rho dW_t^{(1)} + \sqrt{U_t^{-1}} S_t \sqrt{1 - \rho^2} dW_t^{(2)} \\ dU_t &= \tilde{\kappa}(\tilde{\theta} - U_t) dt + \tilde{\varepsilon}\sqrt{U_t} dW_t^{(1)}, \end{cases} \quad (2.2)$$

with $S_0 = s_0$ and $U_0 = 1/v_0$.

Although U is a square-root process, (2.2) is of course not equivalent to the Heston model. Indeed, in the Heston model, it is the diffusion term of S , rather than its inverse, that follows a square-root process. However, the ideas of Kouritzin (2018) can be exploited to obtain an explicit weak solution to (2.2), which will in turn be used to simulate the process.

It is well-known (see for example Hanson (2010)) that if $n := \frac{4\tilde{\kappa}\tilde{\theta}}{\tilde{\varepsilon}^2}$ is a positive integer, the square-root process U is equal in distribution to the sum of n squared Ornstein-Uhlenbeck processes. Proposition 1 below relies on this result.

Proposition 1. *Suppose that $n = \frac{4\tilde{\kappa}\tilde{\theta}}{\tilde{\varepsilon}^2} \in \mathbb{N}^+$ and let $W^{(2)}, Z^{(1)}, \dots, Z^{(n)}$ be independent standard Brownian motions on some probability space $(\Omega, \mathcal{F}, \mathbb{P})$. For $t \geq 0$, define*

$$\begin{aligned} S_t &= s_0 \exp \left\{ \frac{\rho}{\tilde{\varepsilon}} \log \left(\frac{U_t}{U_0} \right) + \left(r + \frac{\rho\tilde{\kappa}}{\tilde{\varepsilon}} \right) t \right. \\ &\quad \left. - \left(\frac{\rho}{\tilde{\varepsilon}} \left(\tilde{\kappa}\tilde{\theta} - \tilde{\varepsilon}^2/2 \right) + \frac{1}{2} \right) \int_0^t U_s^{-1} ds + \sqrt{1 - \rho^2} \int_0^t \sqrt{U_s^{-1}} dW_s^{(2)} \right\}, \\ U_t &= \sum_{i=1}^n \left(Y_t^{(i)} \right)^2, \end{aligned}$$

where

$$Y_t^{(i)} = \frac{\tilde{\varepsilon}}{2} \int_0^t e^{-\frac{\tilde{\kappa}}{2}(t-u)} dZ_u^{(i)} + e^{-\frac{\tilde{\kappa}}{2}t} Y_0^{(i)}, \quad \text{with } Y_0 = \sqrt{U_0/n}$$

and

$$W_t^{(1)} = \sum_{i=1}^n \int_0^t \frac{Y_u^{(i)}}{\sqrt{\sum_{j=1}^n (Y_u^{(j)})^2}} dZ_u^{(i)}.$$

Let $X = (S, U)$, $W = (W^{(1)}, W^{(2)})$ and let $\{\mathcal{F}_t\}_{t \geq 0}$ be the augmented filtration generated by $(W^{(2)}, Z^{(1)}, \dots, Z^{(n)})$. Then,

- $W^{(1)}$ is a standard Brownian motion, and
- (X, W) , $(\Omega, \mathcal{F}, \mathbb{P})$, $\{\mathcal{F}_t\}_{t \geq 0}$ is a weak solution to (2.2).

Proof. We first observe that $Y^{(i)}$, $i \in \{1, \dots, n\}$, are independent Ornstein-Uhlenbeck processes, and that by Lévy's characterization, $W^{(1)}$ is a Brownian motion. It follows from an application of Itô's lemma that

$$\begin{aligned} dU_t &= \sum_{i=1}^n \left(\frac{\tilde{\varepsilon}^2}{4} - \tilde{\kappa} (Y_t^{(i)})^2 \right) dt + \tilde{\varepsilon} Y_t^{(i)} dZ_t^{(i)} \\ &= \left(\frac{n\tilde{\varepsilon}^2}{4} - \tilde{\kappa} \sum_{i=1}^n (Y_t^{(i)})^2 \right) dt + \tilde{\varepsilon} \sum_{i=1}^n Y_t^{(i)} dZ_t^{(i)} \\ &= \left(\frac{n\tilde{\varepsilon}^2}{4} - \tilde{\kappa} U_t \right) dt + \tilde{\varepsilon} \sqrt{U_t} dW_t^{(1)}, \end{aligned} \quad (2.3)$$

where the last equality is obtained by multiplying and dividing the second term on the right-hand side by $\sqrt{\sum_{j=1}^n (Y_t^{(j)})^2}$. Here, since we work under the assumption that $n = \frac{4\tilde{\kappa}\tilde{\theta}}{\tilde{\varepsilon}^2}$, (2.3) can be re-written as

$$dU_t = \tilde{\kappa} (\tilde{\theta} - U_t) dt + \tilde{\varepsilon} \sqrt{U_t} dW_t^{(1)}.$$

An application of Itô's lemma to S_t completes the proof. \square

An alternative, systematic way to verify the functional form for S_t that avoids our Itô-lemma-based guess and verify technique can be found in Kouritzin (2018).

It is likely that for a given market calibration of the 3/2 model, $n = \frac{4\tilde{\kappa}\tilde{\theta}}{\tilde{\varepsilon}^2}$ is not an integer. For this reason, a more general result is needed to develop a simulation algorithm based on an explicit weak solution.

We generalize the definition of n and let $n = \max\left(\lfloor \frac{4\tilde{\kappa}\tilde{\theta}}{\tilde{\varepsilon}^2} + \frac{1}{2} \rfloor, 1\right)$. We further define $\tilde{\theta}_n$ by

$$\tilde{\theta}_n = \frac{n\tilde{\varepsilon}^2}{4\tilde{\kappa}}.$$

It follows that $\tilde{\kappa}\tilde{\theta}_n = \frac{n\tilde{\varepsilon}^2}{4}$.

While U above cannot hit 0 under the Feller condition, it can get arbitrarily close, causing U_t^{-1} to blow up. To go beyond the case $\frac{4\tilde{\kappa}\tilde{\theta}}{\tilde{\varepsilon}^2} \in \mathbb{N}$ treated in Proposition 1, we want to change measures, which is facilitated by stopping U from approaching zero.

This change of measure is needed to readjust the distribution of the paths of U simulated using the (wrong) long-term mean parameter $\tilde{\theta}_n$ and Proposition 1. Indeed, Proposition 1 can be used with $\tilde{\theta}_n$ since $\frac{4\tilde{\kappa}\tilde{\theta}_n}{\tilde{\varepsilon}^2} = n$ is an integer. Under the new measure, the adjusted paths have the correct distribution, that is, the one associated with the desired parameter $\tilde{\theta}$. This idea is made more precise below.

Given a filtered probability space $(\Omega, \mathcal{F}, \{\mathcal{F}_t\}_{t \geq 0}, \hat{\mathbb{P}})$ with independent Brownian motions $Z^{(1)}, \dots, Z^{(n)}$ and $W^{(2)}$, and a fixed $\delta > 0$, we can define $(\hat{S}, \hat{U}) = \{(\hat{S}_t, \hat{U}_t)\}_{t \geq 0}$ by

$$\begin{aligned} \hat{S}_t = s_0 \exp \left\{ \frac{\rho}{\tilde{\varepsilon}} \log(\hat{U}_t/U_0) + \left(r + \frac{\rho\tilde{\kappa}}{\tilde{\varepsilon}} \right) t \right. \\ \left. - \left(\frac{\rho}{\tilde{\varepsilon}} \left(\tilde{\kappa}\tilde{\theta} - \tilde{\varepsilon}^2/2 \right) + \frac{1}{2} \right) \int_0^t \hat{U}_s^{-1} ds + \sqrt{1 - \rho^2} \int_0^t \hat{U}_s^{-1/2} dW_s^{(2)} \right\}, \end{aligned} \quad (2.4)$$

$$\hat{U}_t = \sum_{i=1}^n (Y_t^{(i)})^2, \quad (2.5)$$

and $\tau_\delta = \inf\{t \geq 0 : \hat{U}_t \leq \delta\}$, where

$$Y_t^{(i)} = \frac{\tilde{\varepsilon}}{2} \int_0^{t \wedge \tau_\delta} e^{-\frac{\tilde{\kappa}}{2}(t-u)} dZ_u^{(i)} + e^{-\frac{\tilde{\kappa}}{2}(t \wedge \tau_\delta)} Y_0^{(i)}, \quad \text{with } Y_0 = \sqrt{U_0/n} \quad (2.6)$$

for $i \in \{1, \dots, n\}$.

Theorem 1, to follow immediately, shows that it is possible to construct a probability measure on (Ω, \mathcal{F}) under which (\hat{S}, \hat{U}) satisfies (2.2) until \hat{U} drops below a pre-determined threshold δ .

Theorem 1. *Let $(\Omega, \mathcal{F}, \{\mathcal{F}_t\}_{t \geq 0}, \hat{\mathbb{P}})$ be a filtered probability space on which $Z^{(1)}, \dots, Z^{(n)}, W^{(2)}$ are independent Brownian motions. Let (\hat{S}, \hat{U}) be defined as in (2.4) and (2.5) and let $\tau_\delta = \inf\{t \geq 0 : \hat{U}_t \leq \delta\}$ for some $\delta \in (0, 1)$. Define*

$$\hat{L}_t^{(\delta)} = \exp \left\{ -\frac{\tilde{\kappa}(\tilde{\theta}_n - \tilde{\theta})}{\tilde{\varepsilon}} \int_0^t \hat{U}_v^{-1/2} d\hat{W}_v^{(1)} - \frac{\tilde{\kappa}^2}{2} \left(\frac{\tilde{\theta}_n - \tilde{\theta}}{\tilde{\varepsilon}} \right)^2 \int_0^t \hat{U}_v^{-1} dv \right\} \quad (2.7)$$

with

$$\hat{W}_t^{(1)} = \sum_{i=1}^n \int_0^t \frac{Y_u^{(i)}}{\sqrt{\sum_{j=1}^n (Y_u^{(j)})^2}} dZ_u^{(i)} \quad (2.8)$$

and $\mathbb{P}^\delta(A) = \hat{E}[1_A \hat{L}_T^{(\delta)}] \forall A \in \mathcal{F}_T$ for $T > 0$.

Then, under the probability measure \mathbb{P}^δ , $(W^{(1)}, W^{(2)})$, where

$$W_t^{(1)} = \hat{W}_t^{(1)} + \tilde{\kappa} \frac{\tilde{\theta} - \tilde{\theta}_n}{\tilde{\varepsilon}} \int_0^{t \wedge \tau_\delta} \hat{U}_s^{-1/2} ds,$$

are independent Brownian motions and $(\widehat{S}, \widehat{U})$ satisfies

$$\begin{aligned} d\widehat{S}_t &= \begin{cases} r\widehat{S}_t dt + \widehat{U}_t^{-1/2}\widehat{S}_t \rho dW_t^{(1)} + \widehat{U}_t^{-1/2}\widehat{S}_t \sqrt{1-\rho^2} dW_t^{(2)}, & t \leq \tau_\delta \\ r_\delta \widehat{S}_t dt + \sigma_\delta \widehat{S}_t dW_t^{(2)}, & t > \tau_\delta, \end{cases} \\ d\widehat{U}_t &= \begin{cases} \tilde{\kappa}(\tilde{\theta} - \widehat{U}_t) dt + \tilde{\varepsilon} \widehat{U}_t^{1/2} dW_t^{(1)}, & t \leq \tau_\delta \\ 0, & t > \tau_\delta \end{cases} \end{aligned} \quad (2.9)$$

on $[0, T]$, with

$$\begin{aligned} r_\delta &= r + \frac{\rho}{2\tilde{\varepsilon}\delta} \left(2\tilde{\kappa}\delta - 2\tilde{\kappa}\tilde{\theta} + \tilde{\varepsilon}^2 - \rho\tilde{\varepsilon}^2 \right), \\ \sigma_\delta &= \sqrt{\frac{1-\rho^2}{\delta}}. \end{aligned}$$

Proof. Let $D = \mathcal{S}(\mathbb{R}^2)$, the rapidly decreasing functions. They separate points and are closed under multiplication so they separate Borel probability measures (see Blount and Kouritzin (2010)) and hence are a reasonable martingale problem domain.

To show that $(\widehat{X}, W), (\Omega, \mathcal{F}, \mathbb{P}^\delta), \{\widehat{\mathcal{F}}_t\}_{t \geq 0}$, with $\widehat{X} = (\widehat{S}, \widehat{U})$ and $W = (W^{(1)}, W^{(2)})$, is a solution to (2.9), we show that it solves the martingale problem associated with the linear operator

$$\begin{aligned} \mathcal{A}_t f(s, u) &= \left(r s f_s(s, u) + \tilde{\kappa}(\tilde{\theta} - u) f_u(s, u) + \frac{1}{2} s^2 u^{-1} f_{ss}(s, u) + \rho \tilde{\varepsilon} s f_{su}(s, u) \right. \\ &\quad \left. + \frac{1}{2} \varepsilon^2 u f_{uu}(s, u) \right) \mathbb{1}_{[0, \tau_\delta]}(t) + \left(r_\delta s f_s(s, u) + \frac{1-\rho^2}{2\delta^2} f_{ss} s^2 \right) \mathbb{1}_{[\tau_\delta, T]}(t) \end{aligned}$$

where $f_s = \frac{\partial f(s, u)}{\partial s}$, $f_u = \frac{\partial f(s, u)}{\partial u}$, $f_{ss} = \frac{\partial^2 f(s, u)}{\partial s^2}$, $f_{uu} = \frac{\partial^2 f(s, u)}{\partial u^2}$ and $f_{su} = \frac{\partial^2 f(s, u)}{\partial s \partial u}$. That is, we show that for any function $f \in D$, the process

$$M_t(f) = f(\widehat{S}_t, \widehat{U}_t) - f(\widehat{S}_0, \widehat{U}_0) - \int_0^t (\mathcal{A}_s f)(\widehat{S}_s, \widehat{U}_s) dv,$$

is a continuous, local martingale.

First, we note by (2.4), (2.5), (2.6) as well as Itô's lemma that $(\widehat{S}, \widehat{U})$ satisfies a two-dimensional SDE similar to the 3/2 model (2.2), but with parameters $\kappa, \theta_n, r_\delta$ and $\widehat{r}_t = r - \frac{\tilde{\kappa}\rho}{\tilde{\varepsilon}}(\tilde{\theta} - \widehat{U}_t)\widehat{U}_t^{-1}$. That is, $((\widehat{S}, \widehat{U}), \widehat{W}), (\Omega, \mathcal{F}, \mathbb{P}), \{\widehat{\mathcal{F}}_t\}_{t \geq 0}$, where $\{\widehat{\mathcal{F}}_t\}_{t \geq 0}$ is the augmented filtration generated by $(Z_1, \dots, Z_n, W^{(2)})$, is a solution to

$$d\widehat{S}_t = \begin{cases} \widehat{r}_t \widehat{S}_t dt + \widehat{U}_t^{-1/2} \widehat{S}_t \rho d\widehat{W}_t^{(1)} + \widehat{U}_t^{-1/2} \widehat{S}_t \sqrt{1-\rho^2} dW_t^{(2)}, & t \leq \tau_\delta, \\ r_\delta \widehat{S}_t dt + \sigma_\delta \widehat{S}_t dW_t^{(2)}, & t > \tau_\delta, \end{cases} \quad (2.10)$$

$$d\widehat{U}_t = \begin{cases} \tilde{\kappa}(\tilde{\theta}_n - \widehat{U}_t) dt + \tilde{\varepsilon} \widehat{U}_t^{1/2} d\widehat{W}_t^{(1)}, & t \leq \tau_\delta, \\ 0, & t > \tau_\delta. \end{cases} \quad (2.11)$$

with $\widehat{S}_0 = s_0$, $\widehat{U}_0 = 1/v_0$ and $\widehat{W}^{(1)}$ defined by (2.8). It follows that for any function $f \in D$,

$$\begin{aligned} df(\widehat{S}_t, \widehat{U}_t) &= \mathcal{L}_t f(\widehat{S}_t, \widehat{U}_t) dt \\ &\quad + \left(\rho \widehat{S}_t \widehat{U}_t^{-1/2} f_s(\widehat{S}_t, \widehat{U}_t) + \varepsilon \widehat{U}_t^{1/2} f_u(\widehat{S}_t, \widehat{U}_t) \right) \mathbb{1}_{[0, \tau_\delta]}(t) d\widehat{W}_t^{(1)} \\ &\quad + \left(\widehat{U}_t^{-1/2} \mathbb{1}_{[0, \tau_\delta]}(t) + \delta^{-1/2} \mathbb{1}_{[\tau_\delta, T]}(t) \right) \sqrt{1 - \rho^2} \widehat{S}_t f_s(\widehat{S}_t, \widehat{U}_t) dW_t^{(2)}, \end{aligned} \quad (2.12)$$

where the linear operator \mathcal{L} is defined by

$$\begin{aligned} \mathcal{L}_t f(s, u) &= \left(\widehat{r}_t s f_s(s, u) + \tilde{\kappa}(\tilde{\theta}_n - u) f_u(s, u) + \frac{1}{2} s^2 u^{-1} f_{ss}(s, u) + \rho \varepsilon s f_{su}(s, u) \right. \\ &\quad \left. + \frac{1}{2} \varepsilon^2 u f_{uu}(s, u) \right) \mathbb{1}_{[0, \tau_\delta]}(t) + \left(r_\delta s f_s(s, u) + \frac{1 - \rho^2}{2\delta^2} f_{ss} s^2 \right) \mathbb{1}_{[\tau_\delta, T]}(t). \end{aligned} \quad (2.13)$$

We observe that $\widehat{L}_t^{(\delta)}$ satisfies the Novikov condition, since by definition of \widehat{U}_t ,

$$\frac{|\tilde{\kappa}(\tilde{\theta}_n - \tilde{\theta})|^2}{\varepsilon^2 \widehat{U}_t} \leq \frac{|\tilde{\kappa}(\tilde{\theta}_n - \tilde{\theta})|^2}{\varepsilon^2 \delta},$$

$\widehat{\mathbb{P}}$ -a.s. for all $t \geq 0$. It follows that $\widehat{L}_t^{(\delta)}$ is a martingale and that \mathbb{P}^δ is a probability measure.

We also have from (2.7) and (2.12) that for $f(s, u) \in C^2([0, \infty]^2)$,

$$\left[\widehat{L}^{(\delta)}, f(\widehat{S}, \widehat{U}) \right]_t = \int_0^{t \wedge \tau_\delta} \widehat{L}_v^{(\delta)} \left((r - \widehat{r}_v) \widehat{S}_v f_s(\widehat{S}_v, \widehat{U}_v) + \tilde{\kappa}(\tilde{\theta} - \tilde{\theta}_n) f_u(\widehat{S}_v, \widehat{U}_v) \right) dv. \quad (2.14)$$

Next we define the process $\widehat{M}(f)$ for any $f \in D$ by

$$\begin{aligned} \widehat{M}_t(f) &= \widehat{L}_t^{(\delta)} f(\widehat{S}_t, \widehat{U}_t) - \widehat{L}_0^{(\delta)} f(\widehat{S}_0, \widehat{U}_0) - \int_0^t \widehat{L}_v^{(\delta)} \mathcal{A}_v f(\widehat{S}_v, \widehat{U}_v) dv \\ &= \widehat{L}_t^{(\delta)} f(\widehat{S}_t, \widehat{U}_t) - \widehat{L}_0^{(\delta)} f(\widehat{S}_0, \widehat{U}_0) - \left[\widehat{L}^{(\delta)}, f(\widehat{S}, \widehat{U}) \right]_t - \int_0^t \widehat{L}_v^{(\delta)} \mathcal{L}_v^{(\delta)} f(\widehat{S}_v, \widehat{U}_v) dv. \end{aligned} \quad (2.15)$$

Using integration by parts, we obtain

$$\begin{aligned} \widehat{M}_t(f) &= \int_0^t \widehat{L}_v^{(\delta)} df(\widehat{S}_v, \widehat{U}_v) dv + \int_0^t f(\widehat{S}_v, \widehat{U}_v) d\widehat{L}_v^{(\delta)} - \int_0^t \widehat{L}_v^{(\delta)} \mathcal{L}_v^{(\delta)} f(\widehat{S}_v, \widehat{U}_v) dv \\ &= \int_0^t \widehat{L}_v^{(\delta)} \left[\tilde{\kappa}(\tilde{\theta} - \tilde{\theta}_n) \widehat{U}_v^{-1/2} f(\widehat{S}_v, \widehat{U}_v) + \left(\rho \widehat{S}_v \widehat{U}_v^{-1/2} f_s(\widehat{S}_v, \widehat{U}_v) \right. \right. \\ &\quad \left. \left. + \varepsilon \widehat{U}_v^{1/2} f_u(\widehat{S}_v, \widehat{U}_v) \right) \mathbb{1}_{[0, \tau_\delta]}(v) \right] d\widehat{W}_v^{(1)} \\ &\quad + \int_0^t \widehat{L}_v^{(\delta)} \left(\widehat{U}_v^{-1/2} \mathbb{1}_{[0, \tau_\delta]}(v) + \delta^{-1/2} \mathbb{1}_{[\tau_\delta, T]}(v) \right) \sqrt{1 - \rho^2} \widehat{S}_v f_s(\widehat{S}_v, \widehat{U}_v) dW_v^{(2)} \end{aligned}$$

so $\widehat{M}_t(f)$ is a local martingale. However, since f is rapidly decreasing, $sf_s(s, u)$, $uf_u(s, u)$, $sf_{su}(s, u)$ and $uf_{uu}(s, u)$ are all bounded. We also have that $\widehat{U}_v \geq \delta$ and $\widehat{L}_v^{(\delta)}$ is integrable for all v . Hence, it follows by (2.13), (2.14), (2.15) and Tonelli that $\widehat{M}(f)$ is a martingale.

To finish the proof, it suffices to follow the remark on p.174 of Ethier and Kurtz and show that

$$E \left[\left(f(\widehat{S}_{t_{n+1}}, \widehat{U}_{t_{n+1}}) - f(\widehat{S}_{t_n}, \widehat{U}_{t_n}) - \int_{t_n}^{t_{n+1}} \mathcal{A}_v f(\widehat{S}_v, \widehat{U}_v) dv \right) \prod_{k=1}^n h_k(\widehat{S}_{t_k}, \widehat{U}_{t_k}) \right] = 0, \quad (2.16)$$

for $0 \leq t_1 < t_2 < \dots < t_{n+1}$, $f \in D$, $h \in B(\mathbb{R}^2)$ (the bounded, measurable functions) and where $\widehat{E}[\cdot]$ denotes the $\widehat{\mathbb{P}}$ -expectation. To do so, we re-write the left-hand side of (2.16) as

$$\begin{aligned} & \widehat{E} \left[\widehat{L}_{t_{n+1}}^{(\delta)} \left(f(\widehat{S}_{t_{n+1}}, \widehat{U}_{t_{n+1}}) - f(\widehat{S}_{t_n}, \widehat{U}_{t_n}) - \int_{t_n}^{t_{n+1}} \mathcal{A}_v f(\widehat{S}_v, \widehat{U}_v) dv \right) \prod_{k=1}^n h_k(\widehat{S}_{t_k}, \widehat{U}_{t_k}) \right] \\ &= \widehat{E} \left[\left(\widehat{L}_{t_{n+1}}^{(\delta)} f(\widehat{S}_{t_{n+1}}, \widehat{U}_{t_{n+1}}) - \widehat{L}_{t_n}^{(\delta)} f(\widehat{S}_{t_n}, \widehat{U}_{t_n}) - \int_{t_n}^{t_{n+1}} \widehat{L}_v^{(\delta)} \mathcal{A}_v f(\widehat{S}_v, \widehat{U}_v) dv \right) \prod_{k=1}^n h_k(\widehat{S}_{t_k}, \widehat{U}_{t_k}) \right] \\ &= \widehat{E} \left[\left(\widehat{M}_{t_{n+1}}(f) - \widehat{M}_{t_n}(f) \right) \prod_{k=1}^n h_k(\widehat{S}_{t_k}, \widehat{U}_{t_k}) \right], \end{aligned}$$

which is equal to 0 since $\widehat{M}(f)$ is a martingale. We can then conclude that $(\widehat{S}, \widehat{U})$ solves the martingale problem for \mathcal{A} with respect to $\widehat{\mathbb{P}}$. \square

Remark 1. In Theorem 1, we indicate the dependence of the process $\widehat{L}^{(\delta)}$ on the threshold δ via the superscript. Indeed, $\widehat{L}^{(\delta)}$ depends on δ through \widehat{U} . Going forward, for notational convenience, we drop the superscript, keeping in mind the dependence of the likelihood process on δ .

3. PRICING ALGORITHM

In this section, we show how Theorem 1 can be exploited to price a financial option in the 3/2 model. First, we justify that $(\widehat{S}, \widehat{U})$ defined in (2.4) and (2.5) can be used to price an option in the 3/2 model, even if they satisfy (2.2) only up to τ_δ . We also present an algorithm to simulate paths of $(\widehat{S}, \widehat{U})$ under the 3/2 model as well as the associated importance sampling estimator for the price of the option.

3.1. Importance sampling estimator of the option price. For the rest of this paper, we consider an option with maturity $T \in \mathbb{R}^+$ whose payoff can depend on the whole path of $\{(S_t, V_t)\}_{t \in [0, T]}$, or equivalently, $\{(S_t, U_t)\}_{t \in [0, T]}$. Indeed, since $V_t = U_t^{-1}$ for all $0 \leq t \leq T$ and to simplify exposition, we will keep on working in terms of U , the inverse of the variance process, going forward. We consider a payoff function $\phi_T(S, U)$ with $E[|\phi_T(S, U)|] < \infty$. We call $\pi_0 = E[\phi_T(S, U)]$ the

price of the option and the function ϕ_T , its discounted payoff. For example, a call option, which pays out the difference between the stock price at maturity, S_T , and a pre-determined exercise price K if this difference is positive, has discounted payoff function $e^{-rT} \max(S_T - K, 0)$ and price $E[e^{-rT} \max(S_T - K, 0)]$.

Remark 2. We work on a finite time horizon and the option payoff function ϕ_T only depends on (S, U) up to T . We use the index T to indicate this restriction on (S, U) .

The next proposition shows that it is possible to use (\hat{S}, \hat{U}) , rather than (S, U) , to price an option in the 3/2 model.

Proposition 2. Suppose (S, U) is a solution to the 3/2 model (2.2) on probability space $(\Omega, \mathcal{F}, \mathbb{P})$ and $\tau_\delta = \inf\{t \geq 0 : U_t \leq \delta\}$. Define (\hat{S}, \hat{U}) by (2.4) and (2.5), set $\hat{\tau}_\delta = \inf\{t \geq 0 : \hat{U}_t \leq \delta\}$ for $\delta \in (0, 1)$ and let $\phi_T(S, U)$ be a payoff function satisfying $E[|\phi_T(S, U)|] < \infty$. Then,

$$\lim_{n \rightarrow \infty} E^{1/n}[\phi_T(\hat{S}, \hat{U}) \mathbb{1}_{\{\tau_{1/n} > T\}}] = E[\phi_T(S, U)],$$

where $E^\delta[\cdot]$ denotes the expectation under the measure \mathbb{P}^δ defined in Theorem 1.

Proof. By Theorem 1, (\hat{S}, \hat{U}) satisfies (2.2) on $[0, \tau_{1/n}]$ under the measure $\mathbb{P}^{1/n}$. It follows that

$$E^{1/n}[\phi_T(\hat{S}, \hat{U}) \mathbb{1}_{\{\hat{\tau}_{1/n} > T\}}] = E[\phi_T(S, U) \mathbb{1}_{\{\tau_{1/n} > T\}}].$$

Because U satisfies the Feller condition, $\lim_{n \rightarrow \infty} \mathbb{1}_{\{\tau_{1/n} \leq T\}} = 0$, \mathbb{P} -a.s. and

$$\lim_{n \rightarrow \infty} E^{1/n}[\phi_T(\hat{S}, \hat{U}) \mathbb{1}_{\{\hat{\tau}_{1/n} > T\}}] = \lim_{n \rightarrow \infty} E[\phi_T(S, U) \mathbb{1}_{\{\tau_{1/n} > T\}}] = E[\phi_T(S, U)]$$

by the dominated convergence theorem. □

We interpret Proposition 2 in the following manner: by choosing δ small enough, it is possible to approximate π_0 by $\pi_0^{(\delta)} := E^\delta[\phi_T(\hat{S}, \hat{U}) \mathbb{1}_{\{\tau_\delta > T\}}]$, that is, using (\hat{S}, \hat{U}) rather than (S, U) . The advantage of estimating the price of an option via (\hat{S}, \hat{U}) is that the trajectories can easily be simulated exactly under the reference measure $\hat{\mathbb{P}}$ defined in Theorem 1. In practice, we will show in Section 4 that for reasonable 3/2 model calibrations, it is usually possible to find δ small enough that $E^\delta[\phi_T(\hat{S}, \hat{U}) \mathbb{1}_{\{\tau_\delta > T\}}]$ is almost undistinguishable from π_0 .

In the rest of this section, we explain how $\pi_0^{(\delta)}$ can be approximated with Monte Carlo simulation. As mentioned above, paths of (\hat{S}, \hat{U}) are easily simulated under the reference measure $\hat{\mathbb{P}}$, not under \mathbb{P}^δ . It is therefore necessary to express $\pi_0^{(\delta)}$ using Theorem 1 in the following manner

$$\pi_0^{(\delta)} = E^\delta[\phi_T(\hat{S}, \hat{U}) \mathbb{1}_{\{\tau_\delta > T\}}] = \hat{E}[\hat{L}_T \phi_T(\hat{S}, \hat{U}) \mathbb{1}_{\{\tau_\delta > T\}}]. \quad (3.1)$$

From (3.1) and the strong law of large numbers, we can define $\hat{\pi}_0^{(\delta)}$, an importance estimator for $\pi_0^{(\delta)}$, by

$$\hat{\pi}_0^{(\delta)} = \frac{\sum_{j=1}^N \phi_T(\hat{S}^{(j)}, \hat{U}^{(j)}) \hat{L}_T^{(j)} \mathbb{1}_{\{\tau_\delta^{(j)} > T\}}}{\sum_{j=1}^N \hat{L}_T^{(j)}}, \quad (3.2)$$

where $\{\hat{S}^{(j)}, \hat{U}^{(j)}, \hat{L}^{(j)}\}_{j=1}^N$ are $N \in \mathbb{N}$ simulated paths of $(\hat{S}, \hat{U}, \hat{L})$.

3.2. Simulating sample paths. In light of Proposition 2, we now focus on the simulation of $(\hat{S}_t, \hat{U}_t, \hat{L}_t)_{t \leq \tau_\delta}$. Using (2.4) and (2.6), \hat{S} and Y can easily be discretized for simulation purposes. To simplify the simulation of the process \hat{L} , we write (2.7) as a deterministic function of \hat{U} in Proposition 3 below.

Proposition 3. *Let \hat{L}_t be defined as in Theorem 1, with \hat{U} defined by (2.5). Then, for $t \leq \tau_\delta$, \hat{L}_t can be written as*

$$\hat{L}_t = \exp \left\{ \frac{-(\tilde{\kappa}\tilde{\theta}_n - \tilde{\kappa}\tilde{\theta})}{\tilde{\varepsilon}^2} \left[\log(\hat{U}_t/\hat{U}_0) + \tilde{\kappa}t + \frac{\tilde{\kappa}\tilde{\theta} - 3\tilde{\kappa}\tilde{\theta}_n + \tilde{\varepsilon}^2}{2} \int_0^t \hat{U}_s^{-1} ds \right] \right\}. \quad (3.3)$$

Proof. An application of Itô's lemma to $\log \hat{U}_t$ for $t \leq \tau_\delta$ yields

$$\log(\hat{U}_t/\hat{U}_0) = (\tilde{\kappa}\tilde{\theta}_n - \tilde{\varepsilon}^2/2) \int_0^t \hat{U}_s^{-1} ds - \tilde{\kappa}t + \tilde{\varepsilon} \int_0^t \hat{U}_s^{-1/2} d\widehat{W}_s^{(1)}. \quad (3.4)$$

Isolating $\int_0^t \hat{U}_s^{-1/2} d\widehat{W}_s^{(1)}$ in (3.4) and replacing the resulting expression in (2.7) gives the result. \square

For $t \in [0, T)$ and $h \in (0, T - t)$, for simulation purposes, we can re-write (2.4), (2.6) and (3.3) in a recursive manner as

$$\begin{aligned} \hat{S}_{t+h} = \hat{S}_t \exp \left\{ \frac{\rho}{\tilde{\varepsilon}} \log(\hat{U}_{t+h}/\hat{U}_t) + ah - b \int_t^{t+h} \hat{U}_s^{-1} ds \right. \\ \left. + \sqrt{1 - \rho^2} \int_t^{t+h} \hat{U}_s^{-1/2} dW_s^{(2)}, \right\} \end{aligned} \quad (3.5)$$

$$Y_{t+h}^{(i)} = Y_t^{(i)} e^{-\frac{\tilde{\kappa}}{2}h} + \frac{\tilde{\varepsilon}}{2} \int_t^{(t+h) \wedge \tau_\delta} e^{-\frac{\tilde{\kappa}}{2}(t+h-u)} dZ_u, \quad \text{for } i = 1, \dots, n, \quad (3.6)$$

and

$$\begin{aligned} \hat{L}_{(t+h) \wedge \tau_\delta} = L_t \exp \left\{ c \left(\log(\hat{U}_{(t+h) \wedge \tau_\delta}/\hat{U}_t) + \tilde{\kappa}(h \vee (\tau_\delta - t)) \right. \right. \\ \left. \left. + d \int_t^{(t+h) \wedge \tau_\delta} \hat{U}_s^{-1} ds \right) \right\}, \end{aligned} \quad (3.7)$$

where

$$a = r + \frac{\rho\tilde{\kappa}}{\tilde{\varepsilon}} \quad b = \frac{\rho}{\tilde{\varepsilon}}(\tilde{\kappa}\tilde{\theta} - \tilde{\varepsilon}^2/2) \quad c = -\frac{\tilde{\kappa}\tilde{\theta}_n - \tilde{\kappa}\tilde{\theta}}{\tilde{\varepsilon}^2} \quad d = \frac{\tilde{\kappa}\tilde{\theta} - 3\tilde{\kappa}\tilde{\theta}_n + \tilde{\varepsilon}^2}{2}.$$

We now discuss the simulation of $(\hat{S}_{t+h}, \hat{U}_{t+h}, \hat{L}_{t+h})$ given $(\hat{S}_t, \hat{U}_t, \hat{L}_t)$, as well as $\{Y_t^{(i)}\}_{i=1}^n$. Typically, h will be a small time interval, that is, we consider $h \ll T$. It is easy to see from the above that given $Y_t^{(i)}$, $Y_{t+h}^{(i)}$ follows a Normal distribution with mean $Y_t^{(i)}e^{-\frac{\tilde{\kappa}}{2}h}$ and variance $\frac{\tilde{\varepsilon}^2}{4\tilde{\kappa}}(1 - e^{-h\tilde{\kappa}})$. The simulation of $Y_{t+h}^{(i)}$ given $Y_t^{(i)}$ is thus straightforward. \hat{U}_{t+h} can then be obtained by (2.5) as the sum of the squares of each $Y_{t+h}^{(i)}$, for $i = 1, \dots, n$.

Given simulated values \hat{U}_{t+h} and \hat{U}_t , the term $\int_t^{t+h} \hat{U}_s^{-1} ds$, which appears in both \hat{S}_{t+h} and \hat{L}_{t+h} , can be approximated using the trapezoidal rule by letting

$$\int_t^{t+h} \hat{U}_s^{-1} ds \approx \frac{(\hat{U}_t^{-1} + \hat{U}_{t+h}^{-1})}{2} h. \quad (3.8)$$

More precise approximations to this integral can be obtained by simulating intermediate values \hat{U}_{t+ih}^{-1} for $i \in (0, 1)$ and using other quadrature rules. In Kouritzin (2018) and Kouritzin and MacKay (2020), Simpson's $\frac{1}{3}$ rule was preferred. In this section, we use a trapezoidal rule only to simplify the exposition of the simulation algorithm.

Given that $\hat{U}_{t+h} > \delta$ and once an approximation for the deterministic integral $\int_t^{t+h} \hat{U}_s^{-1} ds$ is calculated, \hat{L}_{t+h} can be simulated using (3.7). To generate a value for \hat{S}_{t+h} , it suffices to observe that conditionally on $\{\hat{U}_s\}_{s \in [t, t+h]}$, $\int_t^{t+h} \hat{U}_s^{-1/2} dW_s^{(2)}$ follows a Normal distribution with mean 0 and variance $\int_t^{t+h} \hat{U}_s^{-1} ds$.

The resulting algorithm produces N paths of $(\hat{S}, \hat{U}, \hat{L})$ and the stopping times τ_δ associated with each path; it is presented in Algorithm 1, in the appendix. These simulated values are then used in (3.2) to obtain an estimate for the price of an option.

4. NUMERICAL EXPERIMENT

4.1. Methods and parameters. In this section, we assess the performance of the pricing algorithm derived from Theorem 1. To do so, we use Monte Carlo simulations to estimate the price of European call options. These Monte Carlo estimates are compared with the exact price of the option, calculated with the analytical expression available for vanilla options in the 3/2 model (see for example Lewis (2000) and Carr and Sun (2007)). More precisely, we consider the discounted payoff function $\phi_T(S, U) = e^{-rT} \max(S_T - K, 0)$ for $K > 0$ representing the exercise price of the option and we compute the price estimate according to (3.2).

The precision of the simulation algorithm is assessed using either the mean square error or the relative mean square error, as indicated. We define the mean square

error by

$$MSE = E[(\pi_0 - \hat{\pi}_0^{(\delta)})^2]$$

and the relative mean square error by

$$RelMSE = \frac{E[(\pi_0 - \hat{\pi}_0^{(\delta)})^2]}{\pi_0},$$

where π_0 is the exact price of the option and $\hat{\pi}_0^{(\delta)}$ is the estimate calculated with (3.2). The expectations above are approximated by calculating the estimates a large number of times and taking the mean over all runs.

Throughout this section, we consider the five parameter sets presented in Table 1. Parameter set 1 (PS1) was used in Baldeaux (2012). Parameter set 2 (PS2) was obtained by Drimus (2012) via the simultaneous fit of the 3/2 model to 3-month and 6-month S&P500 implied volatilities on July 31, 2009. The three other parameter sets are modifications of PS2: PS3 was chosen so that $\frac{4\tilde{\kappa}\tilde{\theta}}{\tilde{\varepsilon}^2} \in \mathbb{N}$, and PS4 and PS5 were selected to have a higher n . Recalling that $n = \max\left(\lfloor \frac{4\tilde{\kappa}\tilde{\theta}}{\tilde{\varepsilon}^2} + \frac{1}{2} \rfloor, 1\right)$ represents the number of Ornstein-Uhlenbeck processes necessary to simulate the variance process, we have that $n = 204$ for PS1, $n = 5$ for PS2 and PS3 and $n = 12$ for PS4 and PS5.

Throughout the numerical experiments, the threshold we use is $\delta = 10^{-5}$. For all parameter sets, the simulated process U never crossed below this threshold. Therefore, any δ below 10^{-5} would have yielded the same results.

TABLE 1. Parameter sets

	S_0	V_0	κ	θ	ε	ρ	r	$4\tilde{\kappa}\tilde{\theta}/\tilde{\varepsilon}^2$
PS1	1	1	2	1.5	0.2	-0.5	0.05	204
PS2	100	0.06	22.84	0.218	8.56	-0.99	0.00	5.25
PS3	100	0.06	18.32	0.218	8.56	-0.99	0.00	5.00
PS4	100	0.06	19.76	0.218	3.20	-0.99	0.00	11.72
PS5	100	0.06	20.48	0.218	3.20	-0.99	0.00	12.00

4.2. Results. In this section, we present the results of our numerical experiments. We first test the sensitivity of our simulation algorithm to n , the number of Ornstein-Uhlenbeck processes to simulate. We then compare the performance of our algorithm to other popular ones in the literature.

4.2.1. Sensitivity to n . We first test the impact of n on the precision of the algorithm. Such an impact was observed in Kouritzin and MacKay (2020) in the context of the Heston model. To verify whether this also holds for the 3/2 model, we consider the first three parameter sets and price at-the-money (that is, $K = S_0$) European call options. For PS1, we follow Baldeaux (2012) and compute the price of a call option with maturity $T = 1$. The exact price of this option is 0.4431. PS2 and PS3 are

used to obtain the price of at-the-money call options with $T = 0.5$, with respective exact prices 7.3864 and 7.0422. In all three cases, the length of the time step used for simulation is $h = 0.02$.

Here, we assess the precision of the algorithm using the relative MSE in order to compare all three parameter sets, which yield vastly different prices. The relative quadratic error is approximated by computing the price estimators 20 times, for $N \in \{5000, 10000, 50000\}$ simulations. The integral with respect to time (see step (3) of Algorithm 1) is approximated using $M \in \{2, 4\}$ sub-intervals and Simpson's $\frac{1}{3}$ rule.

The results of Table 2 show that the precision of the simulation algorithm seem to be affected by n . Indeed, as a percentage of the exact price, the MSE of the price estimator is higher for PS1 than for the other parameter sets. This observation becomes clearer as N increases.

We recall that for PS3, $\frac{4\tilde{\kappa}\tilde{\theta}}{\tilde{\varepsilon}^2}$ is an integer, while this is not the case for PS2. It follows that for this latter parameter set, the weights $\widehat{L}_T^{(j)}$ are all different, while they are all equal to 1 for PS3. One could expect the estimator using uneven weights to show a worse performance due to the possible great variance of the weights. However, in this case, both estimators show similar a performance; the algorithm does not seem to be affected by the use of uneven weights.

Finally, Table 2 shows that increasing M may not significantly improve the precision of the price estimator. Such an observation is important, since adding subintervals in the calculation of the time-integral slows down the algorithm. Keeping the number of subintervals low reduces computational complexity of our algorithm, making it more attractive.

TABLE 2. Relative MSE as a percentage of π_0 .

N	PS1		PS2		PS3	
	$M = 2$	$M = 4$	$M = 2$	$M = 4$	$M = 2$	$M = 4$
5000	0.271	0.316	0.183	0.225	0.239	0.214
10000	0.203	0.158	0.111	0.112	0.172	0.143
50000	0.158	0.135	0.085	0.083	0.067	0.070

4.2.2. Comparison to other algorithms. In this section, we compare the performance of our new simulation algorithm for the 3/2 model to existing ones. The first benchmark algorithm we consider is based on a Milstein-type discretization of the log-price and variance process. The second one is based on the quadratic exponential scheme proposed by Andersen (2007) as a modification to the method of Broadie and Kaya (2006), which we adapted to the 3/2 model. These algorithms are outlined in the appendix.

To assess the relative performance of the algorithms, we price in-the-money ($K/S_0 = 0.95$), at-the-money ($K/S_0 = 1$) and out-of-the-money ($K/S_0 = 1.05$) call options with $T = 1$ year to maturity. The exact prices of the options, which are used to calculate the MSE of the price estimates, are given in Table 3. We consider all

parameter sets with the exception of PS1, since this parametrization requires the simulation of 204 Ornstein-Uhlenbeck process, which makes our algorithm excessively slow. Run times for the calculation of the Monte Carlo estimators using $N = 50,000$ simulations and $M = 2$ subintervals are reported in Table 4.

TABLE 3. Exact prices π_0 of European call options.

K/S_0	$PS2$	$PS3$	$PS4$	$PS5$
0.95	10.364	10.055	11.657	11.724
1	7.386	7.042	8.926	8.999
1.05	4.938	4.586	6.636	6.710

Figures 1 and 2 present the relative MSE of the price estimator as a function of the number of simulations. We note that the parametrizations considered in Figure 1 are such that $\frac{4\tilde{\kappa}\tilde{\theta}}{\tilde{\varepsilon}^2} \notin \mathbb{N}$, while the opposite is true for Figure 2.

Overall, the precision of our weighted simulation algorithm is similar to that of the other two algorithms studied. However, certain parameter sets result in more precise estimates. Figure 1 shows that the MSE is consistently larger with the weighted simulation algorithms than with the benchmark ones for PS2. However, with PS4, the weighted algorithm performs as well as the other two algorithms, or better. We note that for PS2, $n = 5$ while for PS4, $n = 12$. It was observed in Kouritzin and MacKay (2020) in the case of the Heston model that as n increases, the weighted simulation algorithm seems to perform better relatively to other algorithms. This observation also seems to hold in the case of the 3/2 model.

For parametrizations that satisfy $\frac{4\tilde{\kappa}\tilde{\theta}}{\tilde{\varepsilon}^2} \in \mathbb{N}$, such as in Figure 2, we observe that the weighted simulation algorithm is at least as precise, and often more, than the other algorithms. In this case, all the weights \hat{L}_T are even, which tends to decrease the variance of the price estimator and thus, to decrease the relative MSE. It is also interesting to note that in the case of Figure 2, since $\frac{4\tilde{\kappa}\tilde{\theta}}{\tilde{\varepsilon}^2} \in \mathbb{N}$, it is not necessary to simulate $\tau_\delta^{(j)}$ and the trajectories \hat{L}_T . Indeed, in this case, it is possible to simplify the algorithm using Proposition 1, which tends to speed it up.

The run times presented in Table 4 show that in general, our method is slower than Milstein's, but faster than the quadratic exponential approximation of Andersen (2007). While the run times of the two benchmarks we consider are somewhat constant across the different parametrizations we tested, the speed of our method depends on a two factors; the number of Ornstein-Uhlenbeck processes n to simulate and whether or not $\frac{4\tilde{\kappa}\tilde{\theta}}{\tilde{\varepsilon}^2} \in \mathbb{N}$. This second factor explains the minor differences between the run times reported for PS2 and PS3. However, it should be noted that simulating the weights \hat{L} is not particularly time consuming, as they are obtained as a deterministic function of \hat{U} and therefore require no additional simulation. The most significant difference in run times is due to n ; for example, it takes twice as long to obtain a price estimate using PS5 ($n = 12, \frac{4\tilde{\kappa}\tilde{\theta}}{\tilde{\varepsilon}^2} \notin \mathbb{N}$) than PS3 ($n = 5, \frac{4\tilde{\kappa}\tilde{\theta}}{\tilde{\varepsilon}^2} \in \mathbb{N}$). While our method is always faster than the one of Andersen (2007) for the

parametrizations studied, we expect that in certain cases (when n is high), it could become slower. Nonetheless, in those cases, our method should be very precise.

We also remark that, when it is used to simulate Heston prices and volatilities, Milstein's method can lead to poor accuracy, especially when the Feller condition is not respected. In the 3/2 model, the Feller condition is always met, so it is normal to expect Milstein's algorithm to perform well. Indeed, Figures 1 and 2 show that it reaches a similar level of precision as the other methods considered.

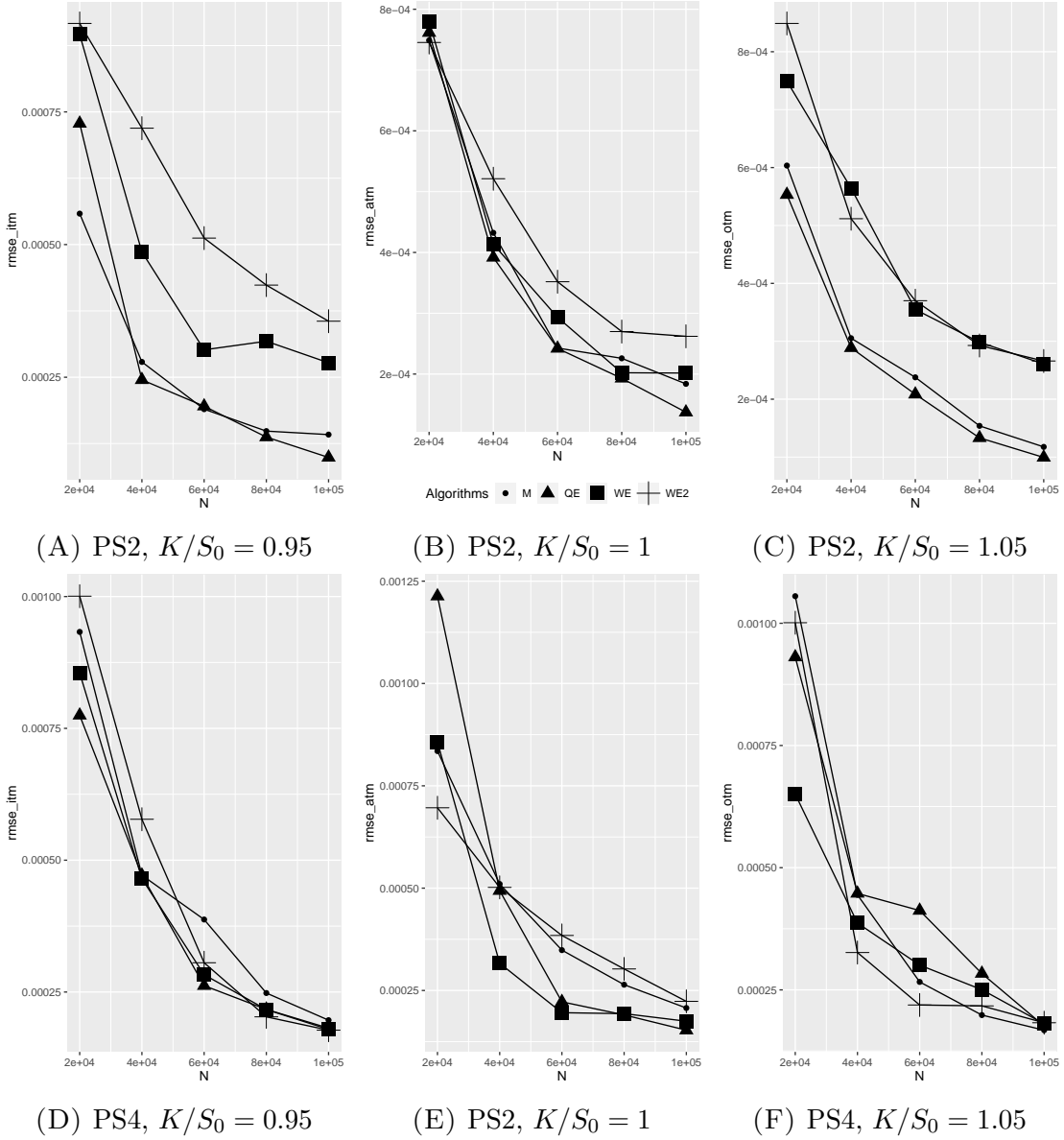


FIGURE 1. Relative MSE as a function of N , PS2 and PS4, algorithms: Milstein (dot), quadratic exponential (triangle), weighted, $M = 2$ (square), weighted, $M = 4$ (cross).

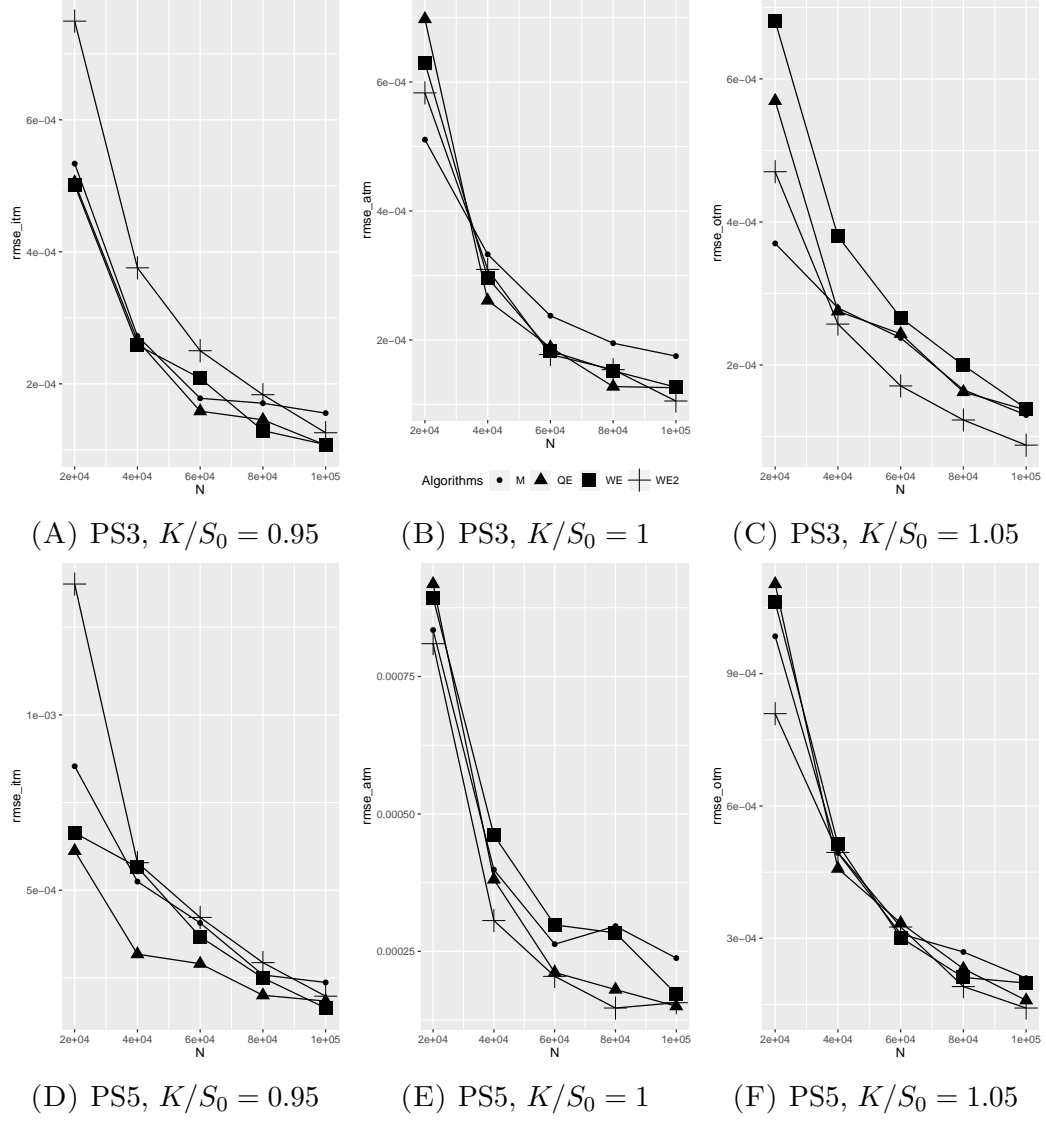


FIGURE 2. Relative MSE as a function of N , PS3 and PS5, algorithms: Milstein (dot), quadratic exponential (triangle), weighted, $M = 2$ (square), weighted, $M = 4$ (cross).

TABLE 4. Run times (in seconds), $N = 5 \times 10^5$, $M = 2$.

Parameters	Milstein	Quadratic exponential	Weighted
PS2	0.445	2.222	0.712
PS3	0.446	2.224	0.615
PS4	0.444	2.226	1.314
PS5	0.444	2.222	1.312

5. CONCLUSION

In this paper, we present a weak explicit solution to the 3/2 model, up until the inverse of the variance process drops below a given threshold. We develop a simulation algorithm based on this solution and show that it can be used to price options in the 3/2 model, since in practice, the inverse variance process stays away from 0. Numerical examples show that our simulation algorithm performs at least as well as popular algorithms presented in the literature. Precision is improved when the parameters satisfy $\frac{4\tilde{\kappa}\tilde{\theta}}{\tilde{\varepsilon}^2} \in \mathbb{N}$ and when n is larger. We also show that it is significantly faster than the quadratic exponential approximation of Andersen (2007) to the method of Broadie and Kaya (2006), which is generally considered to present a good balance between precision and computation time.

It is important to note that the method that we present in this paper could be significantly sped up by the use of sequential resampling, as implemented in Kouritzin and MacKay (2020) for the Heston model. Such improvements, left for future work, could give a significant advantage to our weighted simulation algorithm for the 3/2 model.

APPENDIX

This section presents the simulation algorithms used to produce the numerical examples in Section 4. Algorithm 1 stems from the results we present Theorem 1. Algorithm 2 is a Milstein-type algorithm applied to the 3/2 model. Algorithm 3 is Andersen (2007)'s approximation to the algorithm proposed by Broadie and Kaya (2006), modified for the 3/2 model, since the original algorithm was developed for the Heston model. Algorithms 2 and 3 are considered for comparison purposes.

For all algorithms, we consider a partition $\{0, h, 2h, \dots, mh\}$, with $mh = T$ of the time interval $[0, T]$, and outline the simulation of N paths of $(\hat{S}, \hat{U}, \hat{L})$, as well as the associated stopping times τ_δ .

To simplify the exposition of Algorithm 1, we define the following constants:

$$\alpha_h = e^{-\frac{\tilde{\kappa}}{2}h}, \quad \sigma_h = \frac{\tilde{\varepsilon}^2}{4\tilde{\kappa}} (1 - e^{-h\tilde{\kappa}}).$$

We also drop the hats to simplify the notation.

Algorithm 1 (Weighted explicit simulation).

I. Initialize:

Set the starting values for each simulated path:

$$\{(S_0^{(j)}, L_0^{(j)}, \tau_\delta^{(j)}) = (S_0, 1, T + h)\}_{j=1}^N, \{Y_0^{(l,j)} = \sqrt{U_0/n}\}_{l,j=1}^{n,N}$$

II. Loop on time: for $i = 1, \dots, m$

Loop on particles: for $j = 1, \dots, N$, do

(1) For $l = 1, \dots, n$, generate $Y_{ih}^{(l,j)}$ using $Y_{ih}^{(l,j)} \sim N\left(\alpha_h Y_{(i-1)h}^{(l,j)}, \sigma_h^2\right)$.

(2) Set $U_{ih}^{(j)} = \sum_{l=1}^n (Y_{ih}^{(l,j)})^2$.

- (3) Let $\text{Int}U_{ih}^{(j)} \approx \int_{(i-1)h}^{ih} (U_s^{(j)})^{-1} ds$ using (3.8) (or another quadrature rule).
- (4) Generate $S_{ih}^{(j)}$ from $S_{(i-1)h}^{(j)}$ using (2.4), with $\int_{ih}^{(i-1)h} \widehat{(U_s^{(j)})^{-1/2}} dW_s^{(2)} \sim N(0, \text{Int}U_{ih}^{(j)})$.
- (5) If $ih \leq \tau_\delta^{(j)}$,
 - (i) If $U_{ih}^{(j)} > \delta$, generate $L_{ih}^{(j)}$ from $L_{(i-1)h}^{(j)}$ using (3.7).
 - (ii) Otherwise, set $\tau_\delta^{(j)} = t$.

Algorithm 2 (Milstein).

I. Initialize:

Set the starting values for each simulated path:

$$\{(S_0^{(j)}, U_0^{(j)}) = (S_0, U_0)\}_{j=1}^N$$

II. Loop on time: for $i = 1, \dots, m$

Loop on particles: for $j = 1, \dots, N$, do

- (1) Correct for possible negative values: $\bar{u}^{(j)} = \max(U((i-1)h), 0)$
- (2) Generate $U_{ih}^{(j)}$ from $U_{(i-1)h}^{(j)}$:

$$U_{ih}^{(j)} = U_{(i-1)h}^{(j)} + \tilde{\kappa}(\tilde{\theta} - \bar{u}^{(j)})h + \tilde{\epsilon}\sqrt{\bar{u}^{(j)}h}Z_1^{(j)} + \frac{1}{4}\tilde{\epsilon}^2((Z_1^{(j)})^2 - 1)h,$$

with $Z_1^{(j)} \sim N(0, 1)$.

- (3) Generate $S_{ih}^{(j)}$ from $S_{(i-1)h}^{(j)}$:

$$S_{ih} = S_{(i-1)h} \exp \left\{ \left(r - \frac{1}{2\bar{u}} \right) h + \sqrt{\frac{h}{\bar{u}}} Z_2^{(j)} \right\},$$

with $Z_2^{(j)} \sim N(0, 1)$.

Algorithm 3 (Quadratic exponential).

I. Initialize:

- (1) Set the starting values for each simulated path:

$$\{(S_0^{(j)}, U_0^{(j)}) = (S_0, U_0)\}_{j=1}^N$$

- (2) Fix the constant $\phi_c \in [1, 2]$.

II. Loop on time: for $i = 1, \dots, m$

Loop on particles: for $j = 1, \dots, N$, do

- (1) Set the variables $m_{i,j}$ and $s_{i,j}$:

$$m_{i,j} = \tilde{\theta} + (U_{(i-1)h}^{(j)} - \tilde{\theta})e^{-\tilde{\kappa}h}$$

$$s_{i,j} = \frac{U_{(i-1)h}^{(j)}\tilde{\epsilon}^2 e^{-\tilde{\kappa}h}}{\tilde{\kappa}}(1 - e^{-\tilde{\kappa}h}) + \frac{\tilde{\theta}\tilde{\epsilon}^2}{2\tilde{\kappa}}(1 - e^{-\tilde{\kappa}h})^2$$

(2) Set $\phi_{i,j} = \frac{s_{i,j}^2}{m_{i,j}^2}$.

(3) If $\phi_{i,j} < \phi_c$,
Generate $U_{ih}^{(j)}$ from $U_{(i-1)h}^{(j)}$:

$$U_{ih}^{(j)} = a_{i,j}(b_{i,j} + Z^{(j)})^2,$$

where $Z^{(j)} \sim N(0, 1)$ and

$$b_{i,j}^2 = 2\phi_{i,j}^{-1} - 1 + \sqrt{2\phi_{i,j}^{-1}} \sqrt{2\phi_{i,j}^{-1} - 1}$$

$$a_{i,j} = \frac{m_{i,j}}{1 + b_{i,j}^2}$$

(4) If $\phi_{i,j} \geq \phi_c$,
Generate $U_{ih}^{(j)}$ from $U_{(i-1)h}^{(j)}$:

$$U_{ih}^{(j)} = \frac{1}{\beta} \log \left(\frac{1 - p_{i,j}}{1 - X^{(j)}} \right),$$

where $X^{(j)} \sim \text{Uniform}(0, 1)$ and

$$p_{i,j} = \frac{\psi_{i,j} - 1}{\psi_{i,j} + 1}, \quad \beta_{i,j} = \frac{1 - p_{i,j}}{m_{i,j}}$$

(5) Let $\text{Int}U_{ih}^{(j)} \approx \int_{(i-1)h}^{ih} (U_s^{(j)})^{-1} ds$ using (3.8).

(6) Generate $S_{ih}^{(j)}$ from $S_{(i-1)h}^{(j)}$ using (2.4), with $\int_{ih}^{(i-1)h} \widehat{(U_s^{(j)})^{-1/2}} dW_s^{(2)} \sim N(0, \text{Int}U_{ih}^{(j)})$.

REFERENCES

- D.-H. Ahn and B. Gao. A parametric nonlinear model of term structure dynamics. *The Review of Financial Studies*, 12(4):721–762, 1999.
- L. B. Andersen. Efficient simulation of the Heston stochastic volatility model. *Journal of computational finance*, 11(3):1–42, 2007.
- G. Bakshi, N. Ju, and H. Ou-Yang. Estimation of continuous-time models with an application to equity volatility dynamics. *Journal of Financial Economics*, 82(1): 227–249, 2006.
- J. Baldeaux. Exact simulation of the 3/2 model. *International Journal of Theoretical and Applied Finance*, 15(05):1250032, 2012.
- J.-F. Bégin, M. Bédard, and P. Gaillardetz. Simulating from the heston model: A gamma approximation scheme. *Monte Carlo Methods and Applications*, 21(3): 205–231, 2015.
- D. Blount and M. A. Kouritzin. On convergence determining and separating classes of functions. *Stochastic processes and their applications*, 120(10):1898–1907, 2010.
- M. Broadie and O. Kaya. Exact simulation of stochastic volatility and other affine jump diffusion processes. *Operation Research*, 54(2):217–231, 2006.
- P. Carr and J. Sun. A new approach for option pricing under stochastic volatility. *Review of Derivatives Research*, 10(2):87–150, 2007.

- L. Chan and E. Platen. Pricing and hedging of long dated variance swaps under a 3/2 volatility model. *Journal of Computational and Applied Mathematics*, 278: 181–196, 2015.
- G. G. Drimus. Options on realized variance by transform methods: a non-affine stochastic volatility model. *Quantitative Finance*, 12(11):1679–1694, 2012.
- S. Ethier and T. G. Kurtz. Markov processes: Characterization and convergence, 2005.
- J. Goard and M. Mazur. Stochastic volatility models and the pricing of vix options. *Mathematical Finance: An International Journal of Mathematics, Statistics and Financial Economics*, 23(3):439–458, 2013.
- M. Grasselli. The 4/2 stochastic volatility model: a unified approach for the heston and the 3/2 model. *Mathematical Finance*, 27(4):1013–1034, 2017.
- F. B. Hanson. Stochastic calculus of Heston’s stochastic-volatility model. In *Proceedings of the 19th International Symposium on Mathematical Theory of Networks and Systems—MTNS*, volume 5, 2010.
- S. L. Heston. A simple new formula for options with stochastic volatility. 1997.
- A. Itkin and P. Carr. Pricing swaps and options on quadratic variation under stochastic time change models—discrete observations case. *Review of Derivatives Research*, 13(2):141–176, 2010.
- M. A. Kouritzin. Explicit Heston solutions and stochastic approximation for path-dependent option pricing. *International Journal of Theoretical and Applied Finance*, 21(01):1850006, 2018.
- M. A. Kouritzin and A. MacKay. Branching particle pricers with Heston examples. *International Journal of Theoretical and Applied Finance*, 2020.
- A. Lewis. Option valuation under stochastic volatility with mathematica code, 2000.
- R. Lord, R. Koekkoek, and D. V. Dijk. A comparison of biased simulation schemes for stochastic volatility models. *Quantitative Finance*, 10(2):177–194, 2010.
- C. H. Yuen, W. Zheng, and Y. K. Kwok. Pricing exotic discrete variance swaps under the 3/2-stochastic volatility models. *Applied Mathematical Finance*, 22(5): 421–449, 2015.
- W. Zheng and P. Zeng. Pricing timer options and variance derivatives with closed-form partial transform under the 3/2 model. *Applied mathematical finance*, 23(5):344–373, 2016.

DEPARTMENT OF MATHEMATICS, UNIVERSITÉ DU QUÉBEC À MONTRÉAL, MONTREAL, QC,
H3C 3P8 CANADA

Email address: kouarfate.iro.rene@courrier.uqam.ca

DEPARTMENT OF MATHEMATICAL AND STATISTICAL SCIENCES, UNIVERSITY OF ALBERTA,
EDMONTON, AB, T6G 2G1 CANADA

Email address: michaelk@ualberta.ca

DEPARTMENT OF MATHEMATICS, UNIVERSITÉ DU QUÉBEC À MONTRÉAL, MONTREAL, QC,
H3C 3P8 CANADA

Email address: mackay.anne@uqam.ca